A High-Performance Epitaxial Transparent Oxide Thin-Film Transistor Fabricated at Back-End-Of-Line Temperature (< 450°C) by Suboxide Molecular-Beam Epitaxy

CNF Project Number: 2543-17

Principal Investigator(s): Darrell Schlom

User(s): Jisung Park

Affiliation(s): Department of Material Science and Engineering, Cornell University, Ithaca, NY 14853, USA

Primary Source(s) of Research Funding: Semiconductor Research Corporation

Contact(s): schlom@cornell.edu, gp359@cornell.edu

Primary CNF Tools Used: PT720/740, PVD75 sputter deposition, Autostep i-line stepper

Abstract:

We fabricated a micron-scale field effect transistor (FET) based on epitaxial In_2O_3 thin film with drain current of 0.2 A/mm and on-off ratio of 1×10^8 at room temperature. The whole device manufacturing process including epitaxial In_2O_3 growth takes place below 450°C, making it suitable for back-end-of-line (BEOL) process.

Summary of Research:

Epitaxial layer of indium oxide (In_2O_3) was formed below the threshold for BEOL process, T_{sub} < 450°C, with narrow rocking curve less than 0.05° and low surface roughness of 0.45 nm RMS value, using recently developed version of molecular-beam epitaxy called suboxide MBE [1,2]. At lower carrier concentration regime, an epitaxial In_2O_3 film attained a mobility of 28 $cm^2V^{-1}s^{-1}$ at a carrier concentration of 1.35×10^{19} cm^{-3}. We chose this film to make a FET device because of its low carrier concentration, which is ideal for achieving complete depletion.

We used reactive ion etching using the same conditions we described recently for etching stannate materials for device isolation, and it worked well for In_2O_3 [3]. Contacts at the source/drain and top gate were made with sputtered ITO thin film. For dielectric, ALD-grown HfO_2 was deposited. Figure 1 depicts the device schematic. The characteristics of the devices are shown in Figure 2 and Figure 3.

The hysteresis behavior in the transfer characteristic with respect to the voltage sweep directions is similar to what we saw on $BaSnO_3$-based field effect transistor made with the same technique. It is believed this non-ideal behavior is attributed to the defects in HfO_2. The drain current of the device in the output characteristic is 0.2 A/mm and the on-off ratio is 1×10^8. In Figure 4, we compared the results of our devices to those of the most advanced oxide channel thin film transistor [4-49].

Our result is in the upper left corner, where the expected performance with high drain current and on-off ratio should be found. This indicates that our results are comparable to the best-performing devices based on alternative oxide channel materials, and thus promising.

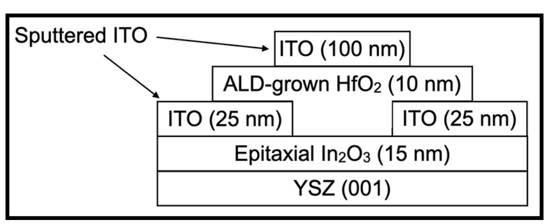

Figure 1: Device schematic.

References:

[1] P. Vogt, et al., APL Materials 9 (2021) 031101.
[2] P. Vogt and O. Bierwagen, Phys. Rev. Mat. 2 (2018) 120401.
[3] J. Park, US Patent 10,868,191 (2020).
[4] Z. Yuan, et al., Thin Solid Films 519, 3254-3258 (2011).
[5] P. K. Nayak, et al., Appl. Phys. Lett. 103, 033518 (2013).
[6] N. Mitoma, et al., Appl. Phys. Lett. 104, 102103 (2014).
[7] L. Wang, et al., 2020 IEEE Symposium on VLSI Technology (2020).
[8] M.Si, et al., IEEE Trans. Electron Devices 68, 1075-1080 (2021).
[9] M. Si, et al., IEEE Electron Device Lett. 42, 184 (2021).
[10] M. Si, et al., Nano Lett. 21, 500-506 (2021).
[11] J. Park, et al., APL Mater. 8, 011110 (2020).
[12] U. Kim, et al., APL Mater. 3, 036101 (2015).
[13] J. Shin, et al., Appl. Phys. Lett. 109, 262102 (2016).
[14] C. Park, et al., Appl. Phys. Lett. 105, 203503 (2014).
[15] Y. M. Kim, et al., APL Mater. 5, 016104 (2017).
[16] Y. M. Kim, et al., Appl. Phys. Exp. 9, 011201 (2016).
[17] Y. Kim, et al., APL Mater. 6, 096104 (2018).
[18] J. Cheng, et al., J. Vac. Sci. Technol. B 38, 012201 (2020).
[19] J. Cheng, et al., IEEE Electron Device Lett. 41. 621 (2020).
[20] J. Cheng, et al., Appl. Phys. Lett. 118, 042105 (2021).
[21] H.-H. Hsieh and C.-C. Wu, Appl. Phys. Lett. 89, 041109 (2006).
[22] E. Fortunato, et al., Adv. Mater. 24, 2945-2986 (2012).
[23] B. Bayraktaroglu, et al., IEEE Electron Device Lett. 30, 946-948 (2009).
[24] B.-Y. Oh, et al., Semicond. Sci. Technol. 26, 085007 (2011).
[25] B. Bayraktaroglu, et al., IEEE Electron Device Lett. 29, 1024-1026 (2008).
[26] K. Nomura, et al., Science 300, 1269-1272 (2003).
[27] K. Nomura, et al., Nature 432, 488-492 (2004).
[28] R. Yao, et al., Appl. Phys. Lett. 112, 103503 (2018).
[29] N. C. Su, et al., IEEE Electron Device Lett. 30, 1317-1319 (2009).
[30] C.-Y. Chung, et al., Appl. Phys. Lett. 106, 123506 (2015) /igzo.
[31] I. Noviyana, et al., Materials 10, 702 (2017).
[32] S. Tomai, et al., Jpn. J. Appl. Phys. 51, 03CB01 (2012).
[33] R. Jany, et al., Adv. Mater. Int. 1, 1300031 (2013).
[34] L. Dong, et al., Proc. IEEE Int. Electron Devices Mtg, 26.4.1-26.4.4. (2010).
[35] H. Zhou, et al., Appl. Phys. Lett. 111, 092102 (2017).
[36] A. J. Green, et al., IEEE Electron Device Lett. 38, 790-793 (2017).
[37] Z. Xia, et al., IEEE Electron Device Lett. 39, 568-571 (2018).
[38] N. Moser, et al., IEEE Electron Device Lett. 38, 775-778 (2017).
[39] K. D. Chabak, et al., IEEE Electron Device Lett. 39, 67-69 (2018).
[40] H. Zhou, et al., ACS Omega 2, 7723.7729 (2017).
[41] N. A. Moser, et al., Appl. Phys. Lett. 110, 143505 (2017).
[42] W. S. Hwang, et al., Appl. Phys. Lett. 104, 203111 (2014).
[43] C. Ju, et al., Curr. Appl. Phys. 16, 300-304 (2016).
[44] R. E. Presley, et al., J. Phys. D: Appl. Phys. 37, 2810-2813 (2004).
[45] S. Li, et al., Nat. Mater. 18, 1091-1097 (2019).
[46] M. Si, et al., ACS Nano 14, 11542-11547 (2020).
[47] J. Zhang, et al., IEEE Electron Device Lett. 40, 1463 (2019).
[48] A. Verma, et al., Appl. Phys. Lett. 105, 113512 (2014).
[49] H. Chandrasekar, et al., ACS Appl. Electron. Mater. 2, 510.516 (2020).

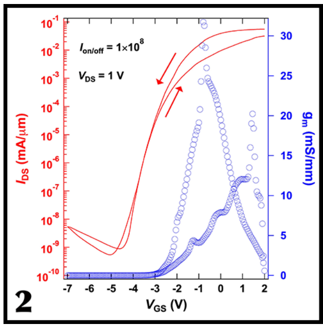

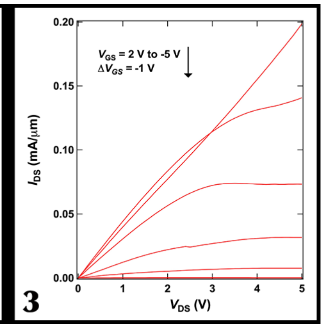

Figure 2, left: Transfer characteristic of the device. Figure 3, right: Output characteristic of the device.

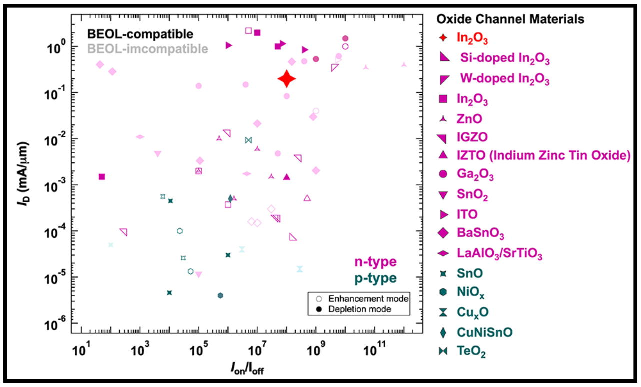

Figure 4: The comparison of device performances based on oxide channel materials in terms of drain current and on-off ratio.